Chinese Journal of
POLYMER SCIENCE

RESEARCH ARTICLE

https://doi.org/10.1007/s10118-024-3102-z
Chinese J. Polym. Sci. **2024**, *42*, 729–738

Research on Bast Fiber Extracted from the White Bark of Three Species in the Genus *Broussonetia*

Shan-Shan Jin[a], Si-Nong Wang[a*], Yan-Yan Huang[a], Jing-Yu Zhang[a], Peng Liu[a], Hui Yu[a], Hong-Dong Zhang[b], and Yu-Liang Yang[a,b*]

[a] *Institute for Preservation and Conservation of Chinese Ancient Books, Fudan University Library, Fudan University, Shanghai 200433, China*
[b] *State key laboratory of Molecular Engineering of polymers, Department of Macromolecular Science, Fudan University, Shanghai 200433, China*

Electronic Supplementary Information

Abstract Against the backdrop of a global paper resource shortage, there is a growing need to identify fast-growing tree species capable of producing long-lasting paper. Three plant species namely *Broussonetia kazinoki*, *Broussonetia papyrifera* and hybrid paper mulberry, belong to the *Broussonetia* genus, were collected from China to study their white bark suitability for pulp and papermaking. Their chemical composition revealed that the holocellulose content in *Broussonetia kazinoki* and *Broussonetia papyrifera* was more than 80%. The molecular weight distribution of several holocellulose/α-cellulose is observed by GPC, which allows us to better observe the changes of various components on the molecular weight. The yield, lignin, whiteness, and molecular weight of the pulps obtained by NaOH treatment were determined. Optical microscope was used to characterize the fiber length-width ratio and rigidity. Finally, the improvement of the fiber rigidity method based on the Kratky-Porod chain model makes it more theoretical and further reveals the influencing factors of fiber rigidity. This study demonstrates the high potentiality of these three species for papermaking applications.

Keywords *Broussonetia* genus; Cellulose; Alkaline pulping; Kratky-Porod chain model; Fiber rigidity

Citation: Jin, S. S.; Wang, S. N.; Huang, Y. Y.; Zhang, J. Y.; Liu, P.; Yu, H.; Zhang, H. D.; Yang, Y. L. Research on bast fiber extracted from the white bark of three species in the genus *Broussonetia*. *Chinese J. Polym. Sci.* **2024**, *42*, 729–738.

INTRODUCTION

As a product of natural polymer fibers, paper played a vital role in human civilization, serving as a medium for recording information and preserving culture.[1] Throughout the long history of papermaking, diverse materials, such as the bark from Moraceae plants, bamboo, straw of rice, and wheat have been utilized, each possessing distinct characteristics. However, paper from inappropriate raw materials often exhibits weakness and brittleness within a few decades.[2] As papermaking techniques advanced, greater care was taken in selecting raw materials, and the pulping process became more complex.[3] Generally, paper with a high molecular weight tends to have a longer lifespan.[4] Meanwhile, the deterioration of forests has posed a significant threat to natural wood resources due to global economic development resulting in a shortage of raw materials for the pulp and paper industry.[5] In this context, there is a need to identify fast-growth plants with high molecular weight of cellulose to produce long-life paper.

The genus of *Broussonetia* is a significant member of the Moraceae family, belonging to the Urticales order and distributed worldwide, including East Asia and the Pacific Islands.[6] This genus encompasses numerous species, primarily including *Broussonetia papyrifera*,[7] *Broussonetia kazinoki*,[8] *Broussonetia kaempferi*, *Broussonetia kurzii*[9] and others. Various parts of plants within this genus, such as fruits, bark, leaves, flowers and roots, hold medicinal properties, while the wood is used in furniture, and the bark is employed in papermaking.[10] Consequently. The genus of *Broussonetia* serves multiple purposes with economic value, attracting increasing attention globally. For this research, we selected three species from the genus of *Broussonetia* as study objects. *Broussonetia kazinoki* (denoted as BK) is a shrub with monoecious flowers, predominantly found in central, south, and southwest provinces and regions of China, as detailed in the publication 'Flora Reipublicae Popularis Sinicae'. Traditionally, BK is utilized in the production of Korean Hanji, crafted from bast fibers of one-year-old BK, boasting cellulose with an exceptionally high average degree of polymerization ranging from 7000–9000.[11] The life expectancy of Hanji paper prepared using historic recipes with BK as raw materials was predicted to be approximately 4000 years.[12] *Broussonetia papyrifera* (denoted as BP) is a tall tree with dioecious flowers. Originat-

* Corresponding authors, E-mail: wangsn@fudan.edu.cn (S.N.W.)
E-mail: yuliangyang@fudan.edu.cn (Y.L.Y.)

Received January 16, 2024; Accepted February 19, 2024; Published online April 3, 2024

ing in Asia, it is now distributed in numerous countries.[13] The use of BP bark for papermaking dates back to the Eastern Han Dynasty of China (A.D. 25–220). Additionally, BP bark serves as the primary ingredient in crafting "tapa" in Tonga, Fijian, and Samoan traditions.[14] Several studies reported the properties of BP bast fiber. For example, the microstructures of BP bast fiber were studied by scanning electron microscope (SEM), and X-ray diffractometer (XRD).[15] The chemical composition and fiber morphology (length and width) of three kinds of artificial cultivation BP were analyzed.[16] Recently researchers used space breeding technology to obtain hybrid *Broussonetia* genus plants with excellent traits. Hybrid paper mulberry (denoted as HPM) in this study, HPM is a hybrid between *Broussonetia kazinoki* and *Broussonetia papyrifera*, with *Broussonetia kazinoki* as the maternal lineage and *Broussonetia papyrifera* as the paternal lineage.[17] HPM has excellent characteristics such as fast growth, high protein content, great adaptability to climates, and multi-resistance to pests and diseases.[18] The leaves of HPM are utilized as a forage, surpassing compound feed due to its ability to reduce the need for antibiotics and improve meat quality.[7] Therefore, it has been widely used in papermaking, ecological restoration, and medicine and livestock.[19,20]

In addition, the fiber rigidity has a significant influence on the effective binding area of the fiber, which is related to the physical and mechanical properties of paper. The reciprocal of fiber rigidity is flexibility. There are various methods have been proposed to characterize fiber rigidity/flexibility. Yan *et al*. measured the free-span length of the fibers used to calculate the flexibility through small deflection beam theory using confocal laser scanning microscopy (CLSM).[21] Pettersson *et al*. reported flexibility data for two types of wet cellulose fibers using a direct force-displacement method using AFM.[22] These methods have complex operating procedures and require expensive equipment. Our previous study proposed a new approach based on the wormlike Kratky-Porod chain model using the optical microscope for fiber rigidity measurement.[23] The method calculated fiber bending rigidity according to the fiber persistence length and the relationship between fiber rigidity and that of cellulose chains inside. It is simple and efficient, with easy operation and low cost measuring dry and wet fibers. And it also has a solid theoretical foundation.[24] However, the Kratky-Porod chain model was used to calculate the fiber persistence length without considering the influence of fiber width. In fact, even for the same fiber, the persistence length is not the same under different widths, so this method was improved in this study.

To the best of our knowledge, limited information exists regarding the molecular structures of cellulose and fiber properties of the white bark from these three species in the genus of *Broussonetia*. This study presents data on their chemical composition, including chemical composition, the molecular structures of holocellulose and *α*-cellulose, the characterization of the pulps in terms of yield, lignin content, whiteness, and as well as the properties of the fibers such as length, width, and fiber rigidity. In addition, the method characterizing fiber rigidity was modified and further revealed the influencing factors of fiber rigidity in this study.

EXPERIMENTAL

Raw Materials

Sodium hydroxide (NaOH), methyl alcohol (MeOH, AR), were purchased from Sinopharm Chemical Reagent Co., LTD. Anhydrous lithium chloride (LiCl, AR), *N*,*N*-dimethylacetamide (DMAc, HPLC), were purchased from Sigma-Aldrich. All reagents used without further purification.

Broussonetia kazinoki, *Broussonetia papyrifera* and hybrid paper mulberry were purchased from Yuanfeng Hemp Products Co., Ltd. in Feicheng (Shandong, China), Guizhou Shiqiao Ancient Method Papermaking Cooperative in Danzhai (Guizhou, China), and Xinsenyuan Agriculture and Forestry Technology Co., Ltd. in Taian (Shandong, China), respectively. The white barks of BK, BP and HPM were used as experimental materials, as shown in Fig. S1 (in the electronic supplementary information, ESI). All types of materials were ground and the 80 mesh fractions were selected to establish their chemical composition using a high-speed mill for chemical component analysis (Photographs are shown in Fig. S1 in ESI). Before pulping, these white barks were cut into 4–5 cm pieces and extensively washed with distilled water to remove the contaminants.

DNA Extraction and Analysis

DNA was extracted from the leaves of three plants with a Plant Genomic DNA Kit (TIANGEN, Beijing,China). Primers is 5'-TCGCATGTACCTGCAGTAGC-3' (rbcl-r) and 5'-ATGTCACCACAAACAGAAAC-3' (rbcl-f). The target sequence was amplified by PCR. PCR products were purified and sequenced by Sangon Biotech Company (Shanghai, China). For sequence comparisons, the BLAST algorithm (www.ncbi.nlm.nih.gov/BLAST) was used, detailed data was shown in Supplementary Material.

Chemical Analysis

The holocellulose of BK, BP and HPM was isolated according to GB/T2677.10-1995. Benzene-ethanol was used to extract 2 g of powder. Then, the powder was infused with 65 mL of distilled (DI) water, 0.5 mL of acetic acid (CH_3COOH) and 0.6 g of sodium chlorite ($NaClO_2$) and placed in 70 °C water bath for 1 h until it turned white. After filtering and washing to neutrality, the mixture was washed three times with acetone and dried in an oven at 105±2 °C to obtain holocellulose (denoted as BK-holocellulose, BP-holocellulose, HPM-holocellulose).

The holocellulose was used to extract *α*-cellulose using the method shown in Kim *et al*.[25] A total of 0.5 g of dried holocellulose was placed into a 100 mL beaker. Then, 12.5 mL of 17.5% NaOH solution was added into the beaker to swell the dried holocellulose. After 45 min, 12.5 mL of DI water (20 °C) was added, and the sample was allowed to sit for 5 min. The sample was filtered using a 1G2 glass filter, and the filtrate was filtered three times. The solid in the glass filter was washed with DI water. Finally, 20 mL of 10% CH_3COOH was added to the residue and the system was kept for 5 min. Finally, after washing to a neutral pH, the residue was dried until a constant weight was reached (denoted as BK-*α*-cellulose, BP-*α*-cellulose, HPM-*α*-cellulose).

The amounts of benzene-ethanol extractible, acid insoluble lignin, acid-soluble lignin and pectin content of samples were assessed by using the following respective GB/T methods: GB/T2677.6-94, GB/T2677.8-94, GB/T10337-2008 and

https://doi.org/10.1007/s10118-024-3102-z

GB/T10742-2008.

Pulping

The pulps of BK, BP and HPM were prepared in 0.01 g/mL NaOH at 100 °C for 30, 45 and 60 min, respectively. The resulting fibers were then washed extensively with water until neutral.

Characterization

Molecular weight distribution

The molecular weight distribution (MWD) was measured by Agilent Technologies gel permeation chromatography (GPC). The cellulose and pulp solutions were injected and chromatographed on two serial columns (Plgel 20um MIXED-A LS, 7.5 × 300 mm). DMAC/LiCl 0.009 g/mL was used as an eluent after filtering through a 0.02 μm filter. This system was connected with an RID (G7162A) detector. MWD and related polymer-relevant parameters were calculated by Cirrus software programs. All the cellulose and pulp solutions were filtered through 0.45 μm poly(tetrafluoroethylene) disposable membranes before GPC analysis.

Aggregation structure

The crystal structure of the cellulose samples was determined by XRD-600 (SHIMADZU, Tokyo, Japan) with CuKα radiation (k=0.154 nm) at 40 kV and 30 mA. The scanning rate was 2 (°)·min^{-1} with a scanning step of 0.02° over the angular range 2θ=5°–40°. The crystallinity index was calculated with the peak height method by using the Eq. (1):

$$\mathrm{CI} = \frac{I_{\mathrm{cry}} - I_{\mathrm{am}}}{I_{\mathrm{cry}}} \tag{1}$$

where I_{cry} is the intensity of the (200) lattice peak at 2θ=22.4° for cellulose I, the (020) lattice peak at 2θ=21.7° for cellulose II, and I_{am} is the intensity attributed to amorphous (at 2θ=18° for cellulose I, and 2θ=16° for cellulose II).

Viscosity-average degree of polymerization

The viscosity-average degree of polymerization of the pulp was measured according to the literature and calculated by Eq. (2).[26] The samples were dissolved in 0.5 mol/L of Cuen at 25 °C and filtered through 0.45 μm membranes. By the gradual dilution of filtrate, the efflux time of a range of concentrations was obtained through the capillary viscometer.

$$\mathrm{DP}_{\eta}^{0.7} = 0.408\,[\eta] \tag{2}$$

ATR-FTIR spectrum analysis

Attenuated total reflection-Fourier transform infrared (ATR-FTIR) spectrum of paper sample was taken on spectrometer equipped with a diamond ATR detector (Bruker). The scan scope was 4000–400 cm^{-1}. The integral in the frequency range 2800–3000 cm^{-1} (αCH) was the normalization factor for all absorbance values.[27] As for the analysis of hydrogen bond, the spectral baseline of O—H stretching vibration in FTIR absorption spectra of different papers in the range of 3800–3000 cm^{-1} was adjusted, and assumed the vibration spectra in accord with Gaussian distribution. Then peak fitting software was used to obtain the three H-bond patterns.

Whiteness

The whiteness was tested according to Chinese standard GB/T 7974-2002 by a colorimeter (ZB-A). Diffuse emission factor of the sample to the main wavelength of blue light (457nm).

Fiber properties

The fiber rigidity was tested according to our previously reported methods, which introduced a worm-like chain model proposed by Kratky-Porod to the pulp and paper.[23] In the continuous Kratky-Porod chain, the mean square end-to-end distance $\langle h^2 \rangle$ can be calculated by

$$\left\langle h^2 \right\rangle = 2aL - 2a^2\left(1 - \exp\left(-\frac{L}{a}\right)\right) \tag{3}$$

where L denotes the contour length of the entire chain, a denotes persistence length. Three different types of pulps were measured and plotted by $\langle h^2 \rangle$ against L, All the data were further processed by curve fitting according to Eq. (3).

According to literature,[19] the bending force constant of fiber ought to be rewritten as:

$$\lambda_{\mathrm{fiber}} \approx n_1 a k_{\mathrm{B}} T \tag{4}$$

where k_{B} denotes the Boltzmann constant, which is equal to 1.38×10^{-23} J/K; T denotes the absolute temperature with unit K; a denotes the persistence length with unit m; the unit of λ is N·m^2; n_1 denotes the maximum number of chains that accommodated in a fiber, can be calculated according to Eq. (5):

$$n_1 \approx \frac{V_0}{V_1} \approx \frac{\pi d^2 L_0}{gqv\left(DP_{\eta}\right)} \tag{5}$$

Native forms cellulose belongs to a monoclinic system with cell dimensions of g=8.35 Å, q=10.3 Å, v=7.9 Å and β=84°. The unit of g, q, v, d and L_0 is m, and DP_{η} is dimensionless. The bending force constant of fibers can be calculated by substituting Eq. (5) into Eq. (4).

RESULTS AND DISCUSSION

Characterization of Chemical Compositions

The chemical composition of three plant fibers has the most significant impact on pulping and paper performance.[28] Table 1 shows the average results of the chemical analyses of the three species used in this study. The holocellulose content of BK (84.6%) and HPM (82.2%) bark is higher than those of hardwoods (eucalyptus), softwood (pine) and annual plants (straw) which is between 70%–80%.[29] The holocellulose content of BP (66.8%) bark is lower compared to BK and HPM bark. A higher content of holocellulose for BK and HPM bark provides more pulp yield and probably strength properties compared with BP. The lignin content of BK, BP and HPM is 2.3%, 2.8% and 2.6% re-

Table 1 Chemical composition of raw fiber materials (%).

Samples	Holocellulose	Lignin	Pentosan	Pectin	Ash	BE [a]
BK-white bast	84.6	2.3	5.9	2.4	2.6	4.7
BP-white bast	66.8	2.8	8.2	9.4	6.8	6.2
HBP-white bast	82.2	2.6	9.9	4.1	4.0	14.6

[a]BE, Benzene-ethanol extractible content

https://doi.org/10.1007/s10118-024-3102-z

spectively, which was appropriate, lower than that in bark of kenaf (14.7%),[30] bark of *Eucalyptus sideroxylon* (13%)[31] and bark of hemp (4%).[5] Lignin is an undesirable polymer, and its removal in pulping requires high amounts of energy and chemicals. It means low lignin content means that the dosage of chemicals can be reduced or the holding time can be shortened, which is in principle advantageous for pulping. Pentosan content represents the total amount of pentose-based carbohydrates in a material, including xylose. The pentosan content of BK, BP and HPM bark was determined in this study to be 5.9%, 8.2%, and 9.9%, respectively. The benzene-ethanol extractible content of HBP (14.6%) was higher than BK (4.7%) and BP (6.2%) bark. The BP has higher pectin (9.4%) than BK (2.4%) and HPM (4.1%) bark. The ash of BK (2.6%), BP (6.8%) and HPM (4.0%) bark at a low level, which cannot be considered as an issue.

Cellulose consists of (1–4)-*β*-D-glucopyranose units linked linearly to form long chains. Observed differences between cellulose samples from various raw materials originate mainly from molecular weight distribution (MWD) and supramolecular structure.[32] We extracted holocellulose and *α*-cellulose samples from three bark samples, and the MWD and supramolecular structure were studied, results shown in Fig. 1 and Table 2. The three holocellulose samples gave a bimodal elution profile consisting of high-molar-mass (HMM) and low-molar-mass (LMM) fractions, which corresponded to cellulose and hemicellulose fractions, respectively (Fig. 1a).[33–35] The BK holocellulose had the highest number-average molar mass (M_n) of 3.52×10^5 and the smallest PDI value of 11.4. The HPM holocellulose had the highest weight-average molecular weight (M_w) of 4.6934×10^6. Indeed, the molar mass values might be influenced by delignification conditions, namely, the number of repetitions of oxidation with $NaClO_2$ at 70 °C. Therefore, the molar masses of cellulose and hemicellulose present in the original plants before delignification should be much higher than those shown in Table 2. In the GPC system, the molar masses of HMM fractions can be more accurately and sensitively determined than those of LMM fraction.[36] Therefore, the HMM fractions can be used for molar mass analysis, based on the assumption that neither residual lignin fragments nor hemicellulose molecules were present in the HMM fractions in the range of 11.5–15.5 min curves in the holocellulose samples. The order of M_n was HPM-holocellulose (2.6589×10^6) > BP-holocellulose (2.566×10^6) > BK-holocellulose (2.0995×10^6) in HMM fraction (Table 2). It can be seen that hemicellulose has a great influence on the calculation of molecular weight, especially for M_n.

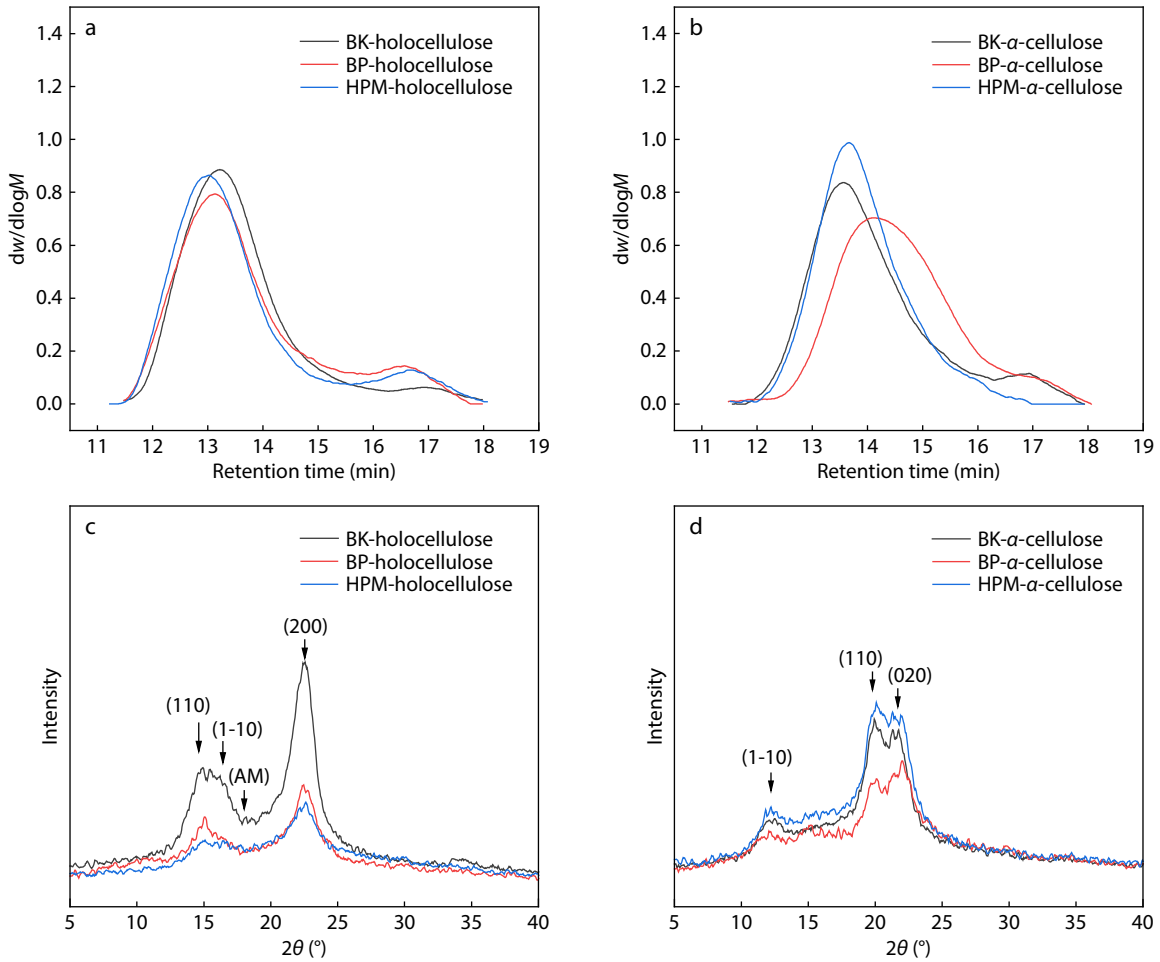

Fig. 1 Characteristics of holocelluloses and *α*-celluloses. (a) Molecular weight distributions of BK, BP and HPM holocellulose; (b) Molecular weight distributions of BK, BP and HPM *α*-cellulose; (c) XRD patterns of BK, BP and HPM holocellulose; (d) XRD patterns of BK, BP and HPM *α*-cellulose.

https://doi.org/10.1007/s10118-024-3102-z

Table 2 Molar mass parameters of holocellulose and *α*-cellulose extracted from BK, BP and HPM.

Samples	M_n [a]	M_w [a]	PDI [b]	CrI [c]
BK-holocellulose	3.52×10^5	4.0194×10^6	11.4	68
BP- holocellulose	2.806×10^5	4.2481×10^6	15.1	61
HPM-holocellulose	2.516×10^5	4.6934×10^6	18.7	53
BK-holocellulose-HMM	2.0995×10^6	5.1616×10^6	2.5	/
BP- holocellulose-HMM	2.566×10^6	5.6551×10^6	2.2	/
HPM-holocellulose-HMM	2.6589×10^6	5.6122×10^6	2.1	/
BK-*α*-cellulose	2.458×10^5	2.2231×10^6	9.0	63
BP-*α*-cellulose	1.84×10^5	1.2781×10^6	6.9	56
HPM-*α*-cellulose	6.668×10^5	2.2003×10^6	3.3	52

[a] M_n and M_w are molar mass, number-average molar mass and weight-average molar mass, respectively (g/mol); [b] PDI obtained by the equation: PDI=M_w/M_n; [c] CrI means Crystallinity Index (%).

Then the *α*-cellulose samples were prepared from holocellulose by soaking in 17.5% NaOH to remove almost all the hemicelluloses. The top peak position of the elution profile for three *α*-cellulose samples shifted to a higher retention time compared to that for holocellulose (Fig. 1b). The HPM-*α*-cellulose sample gave a single peak in the elution profile because the LMM fraction originally present in HPM-holocellulose was mostly removed by treatment with 17.5% NaOH. BK-*α*-cellulose and BP-*α*-cellulose still have small peaks at 16.5–18 min curves in the elution profile. The HPM-*α*-cellulose had the highest M_n of 6.668×10^5 and the smallest PDI value of 3.3, probably because its hemicellulose was removed. The M_n of BK-*α*-cellulose and BP-*α*-cellulose is 2.458×10^5 and 1.84×10^5, respectively. In particular, the M_n of HPM-*α*-cellulose is higher than HPM-holocellulose (ALL fractions) after 17.5% NaOH treatment, which is impossible. If we use the HMM region in HPM-holocellulose for molar mass analysis, the results become more reasonable (the molar mass of *α*-cellulose is lower than holocellulose after 17.5% NaOH treatment). This is probably because the LMM fraction present in HPM-holocellulose caused the average molecular weight to largely decrease.

The supramolecular structure of holocellulose and *α*-cellulose samples were studied by XRD. Figs. 1(c) and 1(d) and Table 2 show the data in the crystallinity calculated based on Eq. (1). Three holocellulose samples exhibit a diffraction pattern typical of cellulose I, with diffraction peaks of the 2θ at 14.5°, 16.5° and 22.4°, which can be assigned to 110, 1-10, and 200 reflections, respectively (Fig. 1c). BK-holocellulose have higher crystallinity (68%) than BP-holocellulose (61%) and HPM-holocellulose (53%). However, the diffractograms of *α*-cellulose exhibit typical diffraction peaks at 2θ=12.2° (1-10), 2θ=19.9° (110) and 2θ=21.7° (020), which is typical of cellulose II (Fig. 1d).[37] It is because that if the concentration of sodium hydroxide is high enough, the native cellulose I transform into Na-cellulose I and further to Na-cellulose II. Na-cellulose I first developed in the amorphous region of cellulose, and the crystalline areas of cellulose I started to transform *via* Na-cellulose I into Na-cellulose II. Cellulose remains in Cellulose II form, both in the crystalline and amorphous regions after washing, this process is called mercerization.[38,39] The crystallinity of BK-*α*-cellulose, BP-*α*-cellulose and HPM-*α*-cellulose is 63%, 56% and 52%, respectively, lower than holocellulose samples.

Characterization of Pulps during the Alkaline Treatment Process

Fibers from bast, are usually treated by alkali, such as hemp, flax, and jute fibers.[40] Sodium hydroxide (0.01 g/mL, 100 °C) was taken on three bark raw materials. First, the yield of pulps was investigated at different alkaline treatment times (Fig. 2a and Table S1 in ESI). After the alkaline treatment for 30 min, the yield values of the BK, BP and HPM pulps are 86%, 80% and 86%, respectively. With the extension of alkaline treatment time, the yield values of three pulps decrease gradually. In detail, after alkaline treatment for 60 min, the BK, BP and HPM pulps declined to 64%, 54% and 57%, respectively. BK and HPM have higher yields than BP during the whole alkaline treatment process because they have higher holocellulose content (Table 1).

The original FTIR spectra of three barks are shown in Fig. S2

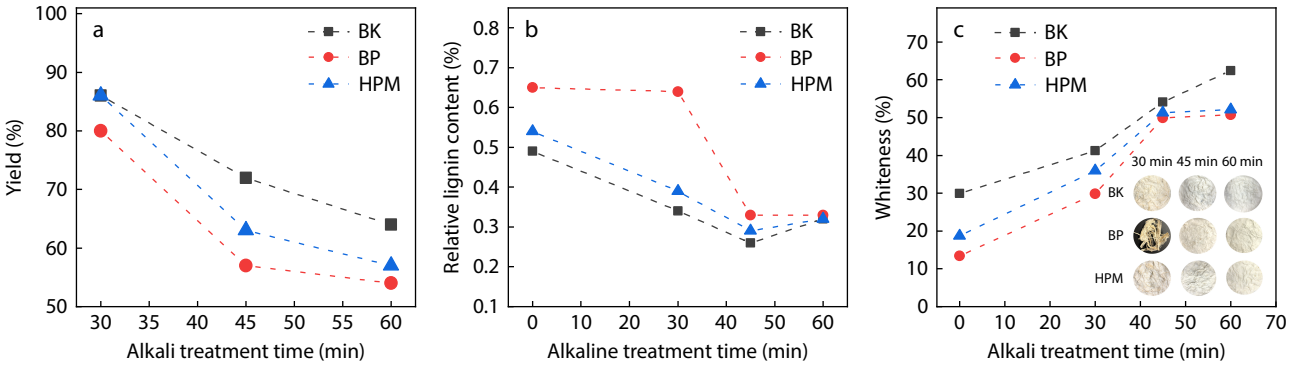

Fig. 2 Characterization of pulps during the alkaline treatment process. (a) Yield of BK, BP and HPM pulp; (b) Relative content of lignin of BK, BP and HPM pulp; (c) Whiteness of BK, BP and HPM pulp.

https://doi.org/10.1007/s10118-024-3102-z

(in ESI). The intensities of aromatic skeletal vibrations (1510 cm^{-1}) and typical bands for carbohydrates (1030 cm^{-1}) were selected for quantitative analysis of lignin and cellulose. The $A_{1510cm^{-1}}/(A_{1510cm^{-1}} + A_{1030cm^{-1}})$ as the relative lignin content. Samples of cellulose and lignin with different contents were used as the standard for the construction of the calibration curve. As shown in Fig. 2(b) and Table S1 (in ESI), the initial relative lignin content value of BK, BP and HPM is 0.49, 0.65 and 0.54, respectively. The order of the relative lignin content in three bark samples is the same as the lignin content measured by chemical method (Table 1). After alkaline treatment for 45 min, the relative lignin content values of three pulps decline in varying degrees. In detail, BP still has the highest relative lignin content of 0.33, followed by HPM (0.29) and BK (0.26). After alkaline treatment for 60 min, the relative lignin content values of BK and HPM increased slightly to 0.32, while BP remained unchanged (0.33). This is probably because after a large amount of lignin is dissolved in the intercellular layer, the cellulose and hemicellulose will also be degraded to different degrees. The decline of lignin in pulp will also cause a change in pulp whiteness. As shown in Fig. 2(c) and Table S1 (in ESI), the BK pups have the highest whiteness during the alkaline treatment process. After the alkaline treatment for 60 minutes, the whiteness of BK pulps increased from 29.9 to 62.4. For BP and HPM pulps, the whiteness values increased between 0–45 min and remained in 45–60 min. This is possible that there are some lignin form chemical linkages with cellulose, which are more difficult to remove and the whiteness is difficult to further increase.[36] Besides, FE-SEM images were performed to visualize changes in the fiber texture during the alkaline treatment process (Fig. S3 in ESI). The offstanding bundles are dissolved and the fiber surface becomes smooth in the course of the alkaline treatment. The surface of BK and HPM fiber becomes smooth at 30 min, while the BP fiber is at 45 min. This phenomenon is consistent with the change of lignin relative content.

The molecular mass parameters of the pulps during the alkaline treatment process are shown in Table 3. With the increase of alkaline treatment time, the M_n and M_w of the three raw materials decreased gradually (BP at 30 min has not formed pulp, which is difficult to dissolve and cannot be tested). It should be pointed out that BP pulp has the largest molecular weight at 45 and 60 min, different from the *α*-cellulose (BP-*α*-cellulose has the lowest molecular weight, shown in Table 2). This is probably because the delignification rate of BP is slower than that of other samples, and the content of pectin is highest in three samples. As a result, the reaction time of cellulose and NaOH in the BP sample is later than that of BK and HPM, so the molecular weight of the BP pulp is higher under the same alkali treatment time. This shows that the molecular weight of the obtained pulp is not only related to the raw material itself but also closely related to the pulp preparation process.

Table 3 Molecular mass parameters of pulps during the alkaline treatment process.

Sample	M_n (g/mol)	M_w (g/mol)	PDI
BK			
30 min	4.5927×10^6	7.0939×10^6	1.54
45 min	3.741×10^6	6.3839×10^6	1.71
60 min	3.4462×10^6	6.1768×10^6	1.80
BP			
30 min	–	–	–
45 min	6.6542×10^6	8.7812×10^6	1.32
60 min	4.7561×10^6	7.3221×10^6	1.54
HPM			
30 min	5.07×10^6	7.9072×10^6	1.60
45 min	4.4834×10^6	7.1537×10^6	1.60
60 min	4.3266×10^6	7.0014×10^6	1.62

Characterization of Fiber Properties

The BK, BP and HBP bark were treated in 1% NaOH at 100 °C for 1 h. Washing them with streaming groundwater until the pH of the solid pulp became neutral and dried at 40 °C. Optical microscope was used to characterize these pulp's fiber properties. First, fiber length had a significant impact on the tearing and tensile strength of paper. The average fiber length of the three pulp samples was 6.62, 5.74 and 6.84 mm, respectively (Table 4). The fiber width of BP (13.23 mm) was the minimum among the three pulp samples. Fig. S4 (in ESI) shows the frequency distribution of the length and width of the fibers. Furthermore, the fiber length-width ratio of three pulps was more than 400, of which BP fibers showed the best suitability (433.86). In general, the length-width ratio for good pulp raw materials needs to reach above 100, and fibers with a high length-width ratio are long, thin and have high tearing resistance.[41]

Then the fiber rigidity was calculated based on the fiber persistence length and the relationship between fiber bending rigidity and that of cellulose chains inside according to our previously reported methods.[23] For cellulosic fiber, $<h^2>$ is described as the average square distance from one end to another end of the fiber. Mass data of three different pulps were measured and plotted by $<h^2>$ against L (Fig. 3). All the data were further processed by curve fitting according to Eq. (3). As shown in Figs. 3(a)–3(c), the determination coefficients of three pulps are all above 0.995 according to Eq. (3), meaning that experimental results are in good agreement with theoretical ones, which can be proven that this model applies to these fibers. The resulting persistence length values of pulp BK, BP and HPM are 3.40, 2.78 and 3.10 mm, respectively. The rigidity of the three fibers is 13.80×10^{-12}, 4.64×10^{-12} and 13.38×10^{-12} $N\cdot m^2$ (Table 4).

Moreover, the elastic coefficient of bending is proportional to the cross-sectional area of the fiber. Therefore, it is neces-

Table 4 Fiber properties of three pulps.

Parameter	L (mm)	a (mm)	d (um)	L/d ratio	DP_η	n_1 ($\times10^{11}$ $N\cdot m^2$)	λ ($\times10^{-12}$ $N\cdot m^2$)	S_0 ($\times10^{-10}$ m^2)	a'' (mm)	λ'' ($\times10^{-12}$ $N\cdot m^2$)	Crystallinity index (%)
BK	6.62	3.40	16.42	403.17	8362	9.87	13.80	2.12	3.43	13.92	79%
BP	5.74	2.78	13.23	433.86	11438	4.06	4.64	1.37	2.66	4.01	67%
HPM	6.84	3.1	17.09	400.23	8803	10.49	13.38	2.29	2.99	12.90	77%

https://doi.org/10.1007/s10118-024-3102-z

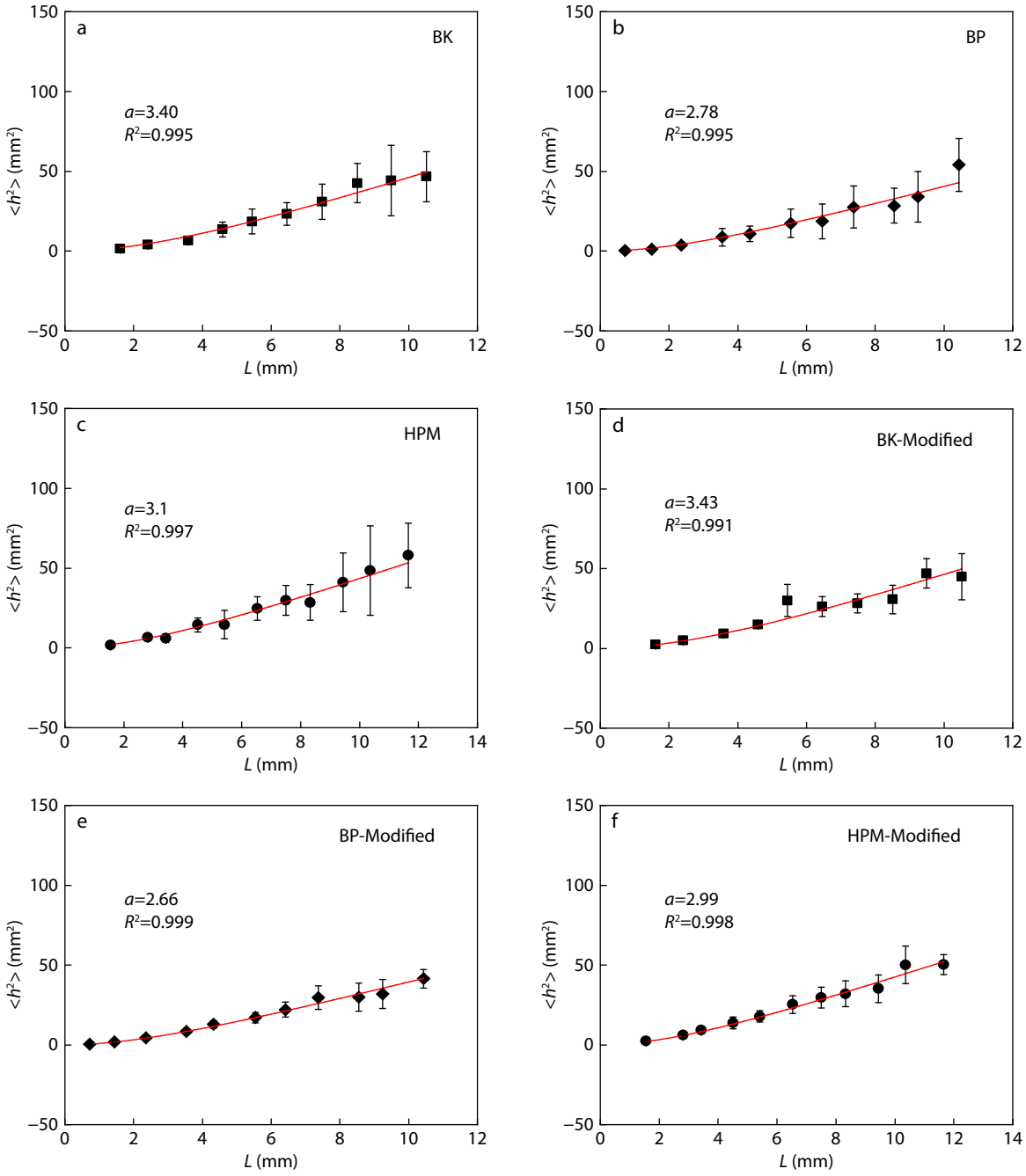

Fig. 3 The application of the Kratky-Porod chain (a–c) and modified (d–f) model in three pulps.

sary to use the fiber cross-sectional area to correct the bending force constant of fiber, and the real fiber rigidity can be further calculated. The mean of fiber cross-sectional area S_0 was selected as the reference state used for calibration.

$$\lambda' = \frac{S_0}{S}\lambda = \frac{S_0}{S}n_1 a k_b T = n_1 a' k_b T \quad (6)$$

Substitute a' into Eq (3), calculate the real mean square end distance $\langle h^2 \rangle$. Each fiber needs to be corrected. Plotting the modified mean square end distance $\langle h^2 \rangle$ against L. All the data were further processed by curve fitting according to Eq. (3) again. The results are shown in Figs. 3(d)–3(f) and Table 4. It can be seen that the curve becomes smooth after modification. The resulting persistence length values a'' of pulp BK, BP and HPM are 3.43, 2.66 and 2.99 mm, respectively. The bending force constant and the fiber rigidity of fibers can be further calculated. In the end, the real rigidity of the pulp BK, BP and HPM pulps is 13.92×10^{-12}, 4.01×10^{-12} and 12.90×10^{-12} N·m². In summary, the BP pulps have the lowest rigidity of three pulps.

Fibers are assembled by fibrils, and the cellulose chains are grouped into fibrils by hydrogen bonds.[42] In the generally accepted that Cellulose I contains one intermolecular H-bond O(6)H…O(3′), two intramolecular H-bonds O(3)H…O(5) and O(2)H…O(6)[43] (Fig. 4a). The hydrogen bonding network of

https://doi.org/10.1007/s10118-024-3102-z

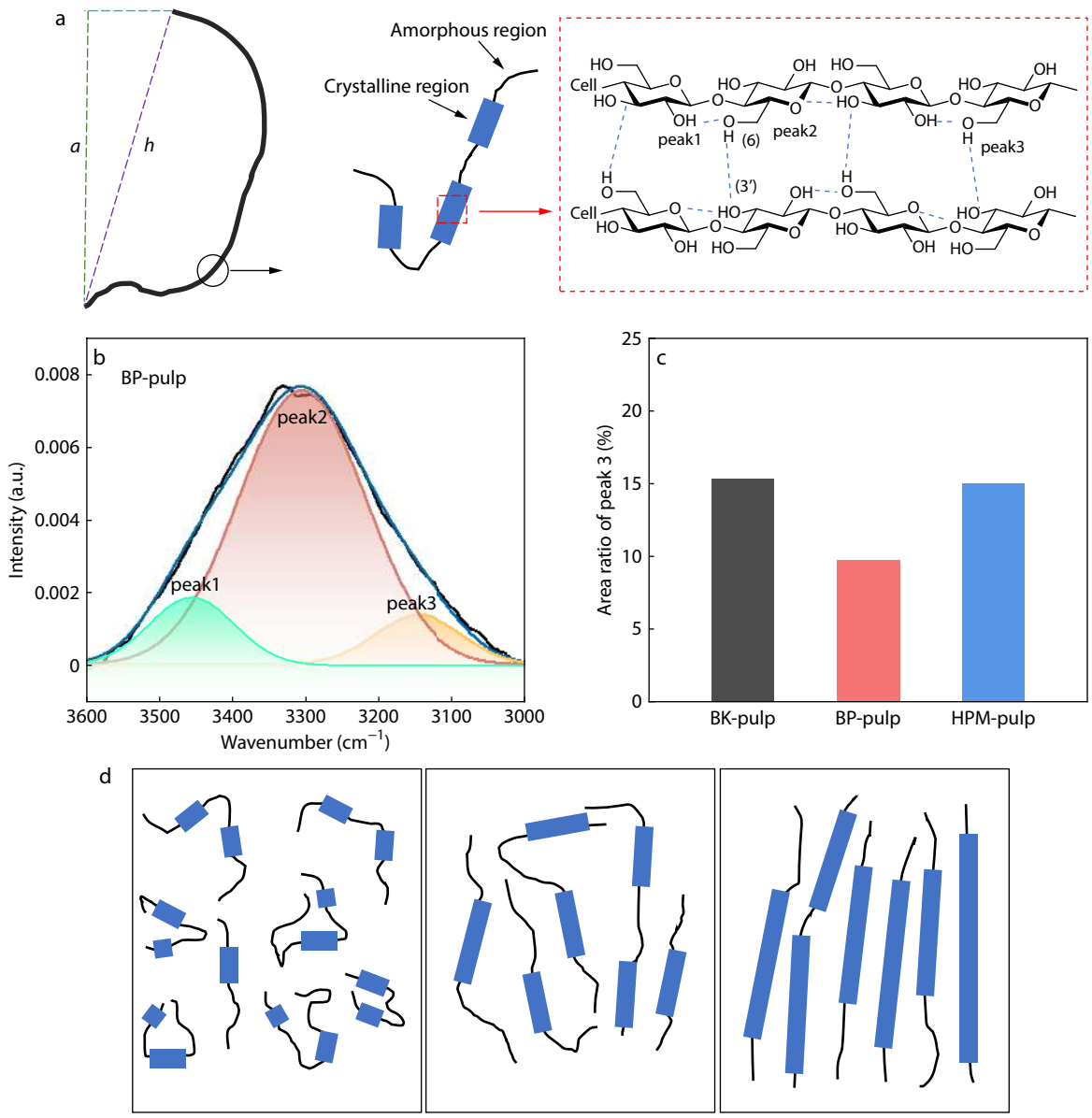

Fig. 4 The intermolecular H-bonds of cellulose and fiber rigidity.

cellulose has been studied with the application of ATR-FTIR, and the peak fitting software was used to obtain the three H-bond patterns (Fig. 4b), detailed data are listed in Table S2 (in ESI). Results showed that the content of intermolecular H-bond O (6)H…O(3′) of BP is lowest (9.75%) in three pulps, which is consistent with the order of fiber rigidity (Fig. 4c). In addition, the crystallinity of BP is 67%, lower than BK (79%) and HPM (77%) (Table 4). As a result, fiber rigidity seems to be related to the crystallinity and content of intermolecular hydrogen bonds. It is probable that with increasing the content of intermolecular H-bond, the crystalline region becomes larger, while rigidity increase (Fig. 4d).

CONCLUSIONS

By study the chemical composition, alkaline pulping, and fiber characterization of three bast fiber, it has been found that the *Broussonetia* genus is an excellent fast-growing wood to solve the shortage of long-fiber in China. The results of chemical compositions indicate that, the bast fiber of *Broussonetia kazinoki* and hybrid paper mulberry have higher holocellulose than *Broussonetia papyrifera,* while all three bast fiber have low lignin. During the alkaline treatment process, *Broussonetia kazinoki* have higher yield and whiteness than hybrid paper mulberry and *Broussonetia papyrifera*, while *Broussonetia papyrifera* have higher molecular mass at same time. The results of fiber length and width distribution of three bast fiber characterized by optical microscope indicate that the fiber with a high length-width ratio (more than 400). Moreover, the method calculated fiber rigidity is further improved by cross-sectional area, making it more theoretical. *Broussonetia papyrifera* bast fiber have a lowest rigidity in three sample. On supramolecular level, *Broussonetia papyrifera* bast fiber have rich intermolecular H-bond content and highest crystallinity. Thus, intermolecular H-bond content and crystallinity is related to the fiber rigidity. It

https://doi.org/10.1007/s10118-024-3102-z

should be noted that the relationship between fiber rigidity and internal microstructure of fibers is worthy to be studied in the future. The present results offer a scientific basis for papermarking.

Conflict of Interests

The authors declare no interest conflict.

Electronic Supplementary Information

Electronic supplementary information (ESI) is available free of charge in the online version of this article at http://doi.org/10.1007/s10118-024-3102-z.

Data Availability Statement

The data that support the findings of this study are available from the author upon reasonable request. The authors' contact information: 20110820003@fudan.edu.cn.

ACKNOWLEDGMENTS

This work was financially supported by the National Key R&D Program of China (No. 2022YFF0904501), and Shanghai Rising-Star Program (No. 23QA1404100).

REFERENCES

1 Buchanan, S. A. The brittle book problem: approaches by research libraries in the United States. *The Paper Conservator* **1987**, *11*, 69–72.
2 Wouters, J. Chemistry: coming soon to a library near you. *Science* **2008**, *322*, 1196–1198.
3 Tsien, T. H. Raw materials for old papermaking in China. *J. Am. Oriental. Soc.* **1973**, *93*, 510–519.
4 Zou, X.; Uesaka, T.; Gurnagul, N. Prediction of paper permanence by accelerated aging I. Kinetic analysis of the aging process. *Cellulose* **1996**, *3*, 243–267.
5 Danielewicz, D.; Surma-Ślusarska, B. Properties and fibre characterisation of bleached hemp, birch and pine pulps: a comparison. *Cellulose* **2017**, *24*, 5173–5186.
6 Chen, Y.; Wang, L.; Liu, X.; Wang, F.; An, Y.; Zhao, W.; Tian, J.; Kong, D.; Zhang, W.; Xu, Y.; Ba, Y.; Zhou, H. The genus *Broussonetia*: an updated review of phytochemistry, pharmacology and applications. *Molecules* **2022**, *27*, 5344–5380.
7 Wang, F.; Su, Y.; Chen, N.; Shen, S. Genome-wide analysis of the UGT gene family and identification of flavonoids in *Broussonetia papyrifera*. *Molecules* **2021**, *26*, 3449-3465.
8 Lee, Y.; Kwon, J.; Jeong, J. H.; Ryu, J. H.; Kim, K. I. Kazinol C from *Broussonetia kazinoki* stimulates autophagy *via* endoplasmic reticulum stress-mediated signaling. *Anim. Cells Syst.* **2022**, *26*, 28–36.
9 Chung, K. F.; Kuo, W. H.; Hsu, Y. H.; Li, Y. H.; Rubite, R. R.; Xu, W. B. Molecular recircumscription of *Broussonetia* (*Moraceae*) and the identity and taxonomic status of B. kaempferi var. australis. *Bot. Stud.* **2017**, *58*, 11–23.
10 Wang, G. W.; Huang, B. K.; Qin, L. P. The genus *Broussonetia*: a review of its phytochemistry and pharmacology. *Phytotherapy Res.* **2012**, *26*, 1–10.
11 Jeong, M. J.; Bogolitsyna, A.; Jo, B. M.; Kang, K. Y.; Rosenau, T.; Potthast, A., Deterioration of ancient Korean paper (Hanji), treated with beeswax: a mechanistic study. *Carbohyd. Polym.* **2014**, *101*, 1249-1254.
12 Jeong, M. J.; Kang, K. Y.; Bacher, M.; Kim, H. J.; Jo, B. M.; Potthast, A. Deterioration of ancient cellulose paper, Hanji: evaluation of paper permanence. *Cellulose* **2014**, *21*, 4621–4632.
13 Lin, J.; Zou, J.; Zhang, B.; Que, Q.; Zhang, J.; Chen, X.; Zhou, W. An efficient *in vitro* propagation protocol for direct organogenesis from root explants of a multi-purpose plant, Broussonetia papyrifera (L.) L'Hér. ex Vent. *Ind. Crop. Prod.* **2021**, *170*, 113686–113695.
14 Whistler, W. A. Broussonetia papyrifera (paper mulberry). *Traditional Tree Initiative.* **2006**, *9*, 1–3.
15 Zhang, T. H.; Cheng, L.; Guo, M.; Zhang, Y. M. Studies on the microstructures and properties of *Broussonetia Papyrifera* fiber. *Appl. Mech. Mater.* **2013**, *481*, 86–91.
16 Li, F.; Li, Y. P.; Zen, Y.; Ma, Y. T.; Zhai, X. X. Fiber morphology and chemical component of Juvenile Wood in three *Broussonetia papyrifera* clones. *J. Henan Agricultural Sci.* **2011**, *40*, 120–122.
17 Zhang, W. A. N.; Yang, G.; Zhao, Y.; Xu, Z.; Huimin, H.; Zhou, J. The chloroplast genome comparative characteristic of artificial breeding tree, a case about *Broussonetia kazinoki* × *Broussonetia papyrifera*. *Biocell*. **2022**, *46*, 803–819.
18 Peng, X.; Teng, L.; Wang, X.; Wang, Y.; Shen, S. *De Novo* assembly of expressed transcripts and global transcriptomic analysis from seedlings of the paper mulberry (*Broussonetia kazinoki* × *Broussonetia papyifera*). *PLoS One* **2014**, *9*, 1–13.
19 Wang, F.; Chen, N.; Shen, S. iTRAQ-based quantitative proteomics analysis reveals the mechanism of golden-yellow leaf mutant in hybrid paper mulberry. *Int. J. Mol. Sci.* **2021**, *23*, 127–145.
20 Pi, Z.; Zhao, M. L.; Peng, X. J.; Shen, S. H. Phosphoproteomic analysis of paper mulberry reveals phosphorylation functions in chilling tolerance. *J. Proteome Res.* **2017**, *16*, 1944–1961.
21 Yan, D.; Li, K. Measurement of wet fiber flexibility by confocal laser scanning microscopy. *J. Mater. Sci.* **2008**, *43*, 2869–2878.
22 Pettersson, T.; Hellwig, J.; Gustafsson, P. J.; Stenström, S. Measurement of the flexibility of wet cellulose fibres using atomic force microscopy. *Cellulose* **2017**, *24*, 4139–4149.
23 Jin, C.; Yu, H.; Wu, C. F.; Zhao, H. B.; Jin, S. S.; Yang, Y. L.; Zhang, H. D. Fiber bending flexibility evaluation by worm-like chain model. *Chinese J. Polym. Sci.* **2022**, *40*, 526–531.
24 Hiromi, Y.; Takenao, Y. in *Helical Wormlike Chains in Polymer Solutions*. Springer, Berlin/Heidelberg, New York, **2016**, Vol. 2E, p21.
25 Kim, S.; Seo, A. Y.; Lee, T. G. Functionalized cellulose to remove surfactants from cosmetic products in wastewater. *Carbohyd. Polym.* **2020**, *236*, 116010–116017.
26 Kes, M.; Christensen, B. E. A re-investigation of the Mark-Houwink-Sakurada parameters for cellulose in Cuen: a study based on size-exclusion chromatography combined with multi-angle light scattering and viscometry. *J. Chromatogr. A* **2013**, *1281*, 32–37.
27 Łojewska, J.; Lubańska, A.; Mikowiec. P.; Iśkowiec. P.; Proniewicz, L. M. FTIR *in situ* transmission studies on the kinetics of paper degradation *via* hydrolytic and oxidative reaction paths. *Appl. Phys. A* **2006**, *83*, 597–603.
28 Marques, G.; Rencoret, J.; Gutiérrez, A.; Río, J. C. Evaluation of the chemical composition of different non-woody plant fibers used for pulp and paper manufacturing. *The Open Agriculture J.* **2010**, *4*, 93–101.
29 Jiménez, L.; Sanchez, I.; Lopez, F. Characterization of Spanish agricultural residues with a view to obtaining cellulose pulp. *Tappi J.* **1990**, *73*, 173–176.
30 Ashori, A.; Harun, J.; Raverty, D. W.; Yusoff, M. N. M. Chemical and morphological characteristics of Malaysian Cultivated Kenaf (*Hibiscus cannabinus*) fiber. *Polym. Plast. Technol. Eng.* **2006**, *45*, 131–134.
31 Miranda, I.; Lima, L.; Quilhó, T.; Knapic, S.; Pereira, H. The bark of Eucalyptus sideroxylon as a source of phenolic extracts with antioxidant properties. *Ind. Crop. Prod.* **2016**, *82*, 81–87.

32 Schult, T.; Hjerde, T.; Odd Inge Optun ; Kleppe, P. J.; Moe, S. Characterization of cellulose by SEC-MALLS. *Cellulose* **2002**, *9*, 149–158.
33 Ono, Y.; Funahashi, R.; Saito, T.; Isogai, A. Investigation of stability of branched structures in softwood cellulose using SEC/MALLS/RI/UV and sugar composition analyses. *Cellulose* **2018**, *25*, 2667–2679.
34 Yanagisawa, M.; Isogai, A. Size exclusion chromatographic and UV-Vis absorption analyses of unbleached and bleached softwood kraft pulps using LiCl/1,3-dimethyl-2-imidazolidinone as a solvent. *Holzforschung* **2007**, *61*, 236–241.
35 Ono, Y.; Isogai, A. Analysis of celluloses, plant holocelluloses, and wood pulps by size-exclusion chromatography/multi-angle laser-light scattering. *Carbohyd. Polym.* **2021**, *251*, 117045–117059.
36 Ono, Y.; Nakamura, Y.; Zhou, Y.; Horikawa, Y.; Isogai, A. Linear and branched structures present in high-molar-mass fractions in holocelluloses prepared from chara, haircap moss, adiantum, ginkgo, Japanese cedar, and eucalyptus. *Cellulose* **2021**, *28*, 3935–3949.
37 Nomura, S.; Kugo, Y.; Erata, T. ^{13}C NMR and XRD studies on the enhancement of cellulose II crystallinity with low concentration NaOH post-treatments. *Cellulose* **2020**, *27*, 3553–3563.
38 Okano, T.; Sarko, A. Mercerization of Cellulose. I. X-ray diffraction evidence for intermediate structures. *J. Appl. Polym. Sci.* **1984**, *29*, 4175–4182.
39 Okano T.; Sarko, A. Mercerization of cellulose 2. Alkali-cellulose intermediates and a possible mercerization mechanism. *J. Appl. Polym. Sci.* **1985**, *30*, 325–332.
40 Mwaikambo, L. Y.; Ansell, M. P. Chemical modification of hemp, sisal, jute, and kapok fibers by alkalization. *J. Appl. Polym. Sci*. **2002**, *84*, 2222–2234.
41 Zhan, H.; Xie, D.; Li, M.B.; Li, J.; Yu, L.; Wang, C.; Wang, S. Fiber properties and chemical compositions of sheaths from three selected sympodial bamboo species as raw materials for papermaking in Yunnan of China. *Eur. J. Wood. Wood. Prod*. **2022**, *81*, 815–818.
42 Lavoine, N.; Desloges, I.; Dufresne, A.; Bras, J. Microfibrillated cellulose – Its barrier properties and applications in cellulosic materials: a review. *Carbohyd. Polym.* **2012**, *90*, 735–764.
43 Yuan, L.; Wan, J.; Ma, Y.; Wang, Y.; Huang, M.; Chen, Y. The content of different hydrogen bond models and crystal structure of *Eucalyptus* fibers during beating. *Bioresources* **2013**, *8*, 717–737.

https://doi.org/10.1007/s10118-024-3102-z